Trade-off performance analysis of Radcom using the relative entropy

1st Yousef Kloob
Dept. of Elect. and Electron. Eng.
University of Manchester
Manchester, UK
Yousef.kloob@manchester.ac.uk

2nd Mohammad Al-Jarrah
Dept. of Elect. and Electron. Eng.
University of Manchester
Manchester, UK
mohammad.al-jarrah@manchester.ac.uk

3rd Emad Alsusa
Dept. of Elect. and Electron. Eng.
University of Manchester
Manchester, UK
e.alsusa@manchester.ac.uk

4th Christos Masouros
Dept. of Elect. and Electron. Eng.
University College London
London, UK
c.masouros@ucl.ac.uk

***Abstract*—n this paper, we analyze the performance trade-off between integrated radar and communications (RadCom) systems using the Kullback-Leibler divergence (KLD) measure, also called the relative entropy (RE). Specifically, we derive the KLD measure for both subsystems for a base-station serving a number of communication users while detecting multiple targets simultaneously. We evaluate the trade-off between the radar and the communication systems using a weighted KLD that can enhance the flexibility of the allocations. The results demonstrate that the KLD is an effective mean for achieving the optimal trade-off between both systems and that it provides a higher degree of controllablity and adaptability for RadCom systems.**

***Index Terms*—Radar and communication (Radcom) systems, multiple-input-multiple-output (MIMO), zero-forcing (ZF), Kullback–Leibler divergence, Separated deployment, Relative Entropy.**

I. Introduction

WITHIN the rapidly progressing sphere of communication technology, the shift towards the 6G era emerges as a defining juncture. This imminent phase in wireless communications isn't just a nominal step-up from its predecessors but rather is set to introduce a paradigm shift in how we perceive and engage with connectivity [1]–[4]. From harnessing the power of holographic communications to designing intelligent energy frameworks, the prospects that 6G presents to us are nothing short of revolutionary. A focal topic of interest in these discussions is the blend of radar functionalities into traditional communication structures, giving birth to the Radcom paradigm.

The intrigue surrounding Radcom systems is not merely theoretical. They present a pathway towards maximizing the efficacy of both physical resources and network bandwidth, hinting at an optimized future for communication architectures [5]–[10]. In this exploration, our attention is riveted towards separated antenna deployment, a method where base station (BS) antennas are earmarked for designated subsystems. Current literature lacks an exhaustive probe into the comparative strengths or potential limitations of this approach.

Clearly, RadCom systems are expected to be a cornerstone in the next-generation wireless ecosystem. An examination of literature works, reveals that the performance metrics for RadCom systems have been using bit error rate for communication functionalities and detection probability for radar systems. The need to combine these evaluation measures into a unified benchmark is evident, especially when for doing a holistic resource management. In response to this challenge, our research draws cues from our prior findings in [11], [12] to introduce a unified performance metric harnessing the Kullback–Leibler divergence (KLD) commonly known as relative entropy (RE), this metric is derived in these papers for each subsystem and it proves the relation between the KLD and commonly used measures such as the Bit Error Rate (BER) for the communication system, and the probability of detection for the radar. While the RE has already etched its mark in radar system studies, its potential utility in the MIMO communication domain is still largely an uncharted territory. Advocating for a unified system performance, we present the KLD as a viable metric that can guide comprehensive system design and resource allocation decisions [13], [14]. This paper delves into a detailed system framework for separated antenna deployment Radcom system, obtaining the KLD closed form for the radar that is much more computationally efficient than found in literature, using the weighted KLD average we present different trade-offs and the high adaptability of this system. One of the important features of our research pivots around the derivation and utilization of this KLD metric, emphasizing on the performance trade-offs inherent between the dual subsystems.

The remainder of this paper is organised as follows. In section II, the system model is presented. Section III we derive the radar KLD, the communication system's KLD, and the weighted average KLD for separated antenna deployment

Radcom system. In section IV, the numerical results are presented, and Section V concludes the work.

Notation: The following notations are used in this paper. Bold uppercase letters (e.g. $\mathbf{S}$) specify matrices, while bold lowercase letters (e.g. $\mathbf{s}$) specify vectors. Superscripts $(\cdot)^*$, $(\cdot)^T$ and $(\cdot)^H$ specify the conjugate, transpose and Hermitian transpose, respectively. Subscripts $(\cdot)_{\mathrm{c}}$ and $(\cdot)_{\mathrm{r}}$ relate the corresponding parameter to the communication or radar system, respectively. The absolute value and the trace operator are denoted by $|\cdot|$ and $\mathrm{tr}\{\cdot\}$, respectively.

II. System Model

We consider a multi-user multi-target (MUMT) MIMO setup. In the proposed Radcom system model, an N-antenna MIMO-BS is considered. These antennas are dual-purpose: they detect T radar targets and simultaneously serve K single-antenna communication user equipments (UEs) in the downlink. Our exploration encompasses the separated antenna deployment, as depicted in Fig.1. The BS is equipped with

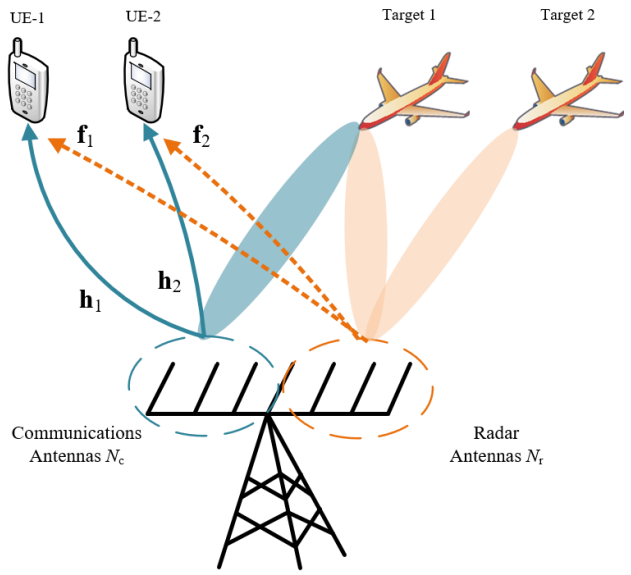

Fig. 1. An illustration diagram for separated deployment Radcom system with two user equipment's, and two targets

a total transmit power of P_{T}, which is strategically allocated between sensing and data communication tasks. This power is judiciously distributed between sensing and data communication tasks. The segments of power designated to the radar and communication functions are represented as P_{r} and P_{c} respectively, confirming that $P_{\mathrm{T}} = P_{\mathrm{c}} + P_{\mathrm{r}}$. At the BS, the Zero-Forcing (ZF) beamforming technique is applied, precoding the data for communication UEs and thus eliminating potential interference between signals [15].

The radar waveform is designed to have a covariance matrix,

$$\mathbf{R}_x \in \mathbb{C}^{N_{\mathrm{r}} \times N_{\mathrm{r}}} \triangleq \frac{1}{L} \sum_{l=1}^{L} \mathbf{x}_l \mathbf{x}_l^H, \tag{1}$$

where L is the overall snapshot count, and $\mathbf{x}_l \in \mathbb{C}^{N_{\mathrm{r}} \times 1}$ is the radar waveform vector for the l-th snapshot.

As shown in Fig.1 for the separated deployment antenna model, the MIMO-BS antennas are divided into two subsets. The first subset contains a number of N_{r} antennas applied for detecting T number of radar targets, whereas the second one utilises the remaining $N_{\mathrm{c}} = N - N_{\mathrm{r}}$ to serve K number of single-antenna communication user equipments (UEs) in the downlink.

A. Communication System

At each instance l, a data symbol $s_{k,l}$ intended for the k-th UE is selected from a normalized constellation, satisfying $\mathbb{E}[|s_{k,l}|^2] = 1$. Given the channel matrix from MIMO-BS to UEs, $\mathbf{H}_l$, these symbols, i.e., $s_{k,l} \forall k$, are precoded using a ZF precoder with a precoding matrix $\mathbf{W}_{\mathrm{c},l} \in \mathbb{C}^{N_{\mathrm{c}} \times K}$ that is normalised using instantaneous matrix normalisation scheme as follows,

$$\mathbf{W}_{\mathrm{c},l} = \frac{\tilde{\mathbf{W}}_{\mathrm{c},l}}{\sqrt{\mathbf{s}_l^H \, \tilde{\mathbf{W}}_{\mathrm{c},l} \, \tilde{\mathbf{W}}_{\mathrm{c},l}^H \, \mathbf{s}_l}} \tag{2}$$

where $\tilde{\mathbf{W}}_{\mathrm{c},l} = \mathbf{H}_l^H \left(\mathbf{H}_l \, \mathbf{H}_l^H\right)^{-1}$ is the non-normalised ZF precoding matrix. This normalization approach ensures that the communication system transmit power satisfies the allocated power. The received signal $\mathbf{y}_l \in \mathbb{C}^{K \times 1}$, at the l-th instance, can be shown as follows,

$$\mathbf{y}_l = \mathbf{D}_{\mathrm{c}} \, \mathbf{H}_l^T \, \mathbf{W}_{\mathrm{c},l} \, \mathbf{P}_{\mathrm{c}} \, \mathbf{s}_l + \mathbf{D}_{\mathrm{c}} \sqrt{\frac{P_{\mathrm{r}}}{N_{\mathrm{r}}}} \mathbf{F}_l^T \mathbf{x}_l + \mathbf{n}_l, \tag{3}$$

where $\mathbf{P}_{\mathrm{c}} = \mathrm{diag}(P_{\mathrm{c},1}, P_{\mathrm{c},2}, \cdots, P_{\mathrm{c},K})$ is a power control matrix for UEs, $\mathbf{H}_l \in \mathbb{C}^{N_{\mathrm{c}} \times K} \sim \mathcal{CN}\left(0, 2\sigma_H^2\right)$ is the BS-UEs communication channel matrix which is modeled as flat Rayleigh fading, $\mathbf{F}_l^T \in \mathbb{C}^{N_{\mathrm{r}} \times T} \sim \mathcal{CN}\left(0, 2\sigma_F^2\right)$ is the radar-communication interference channel matrix modeled as flat Rayleigh fading from the radar antennas to each of the UEs, and $\mathbf{n}_l \in \mathbb{C}^{K \times 1} \sim \mathcal{CN}\left(0, 2\sigma_n^2\right)$ is the additive white Gaussian noise (AWGN). The matrix $\mathbf{D}_{\mathrm{c}} = \mathrm{diag}(d_{\mathrm{c},1}^{-\eta/2}, d_{\mathrm{c},2}^{-\eta/2}, \cdots, d_{\mathrm{c},K}^{-\eta/2})$ accounting for the free space pathloss, where η is the pathloss exponent, and $d_{\mathrm{c},k}$ is the k-th UE distance to BS. Throughout the paper, the channels are assumed to be independent and identically distributed (iid).

B. Radar System

We consider a scenario where each target resides in a unique radar bin [16], [17], enabling clear differentiation of the target count in the environment. It should be highlighted that the literature offers several algorithms designed for the separation of signals linked to distinct targets, particularly in scenarios involving indistinguishable targets. These methods enable an accurate estimation of the number of targets present, [18]–[20]. It is assumed that the BS is informed of the potential target count based on past records. Nonetheless, a straightforward enumeration technique can be implemented by utilizing the detection methodology presented in this paper across all angular-range-Doppler radar segments, followed by an enumeration of the identified targets. MIMO radar capabilities

include the concurrent generation of multiple beams through the amalgamation of orthogonal signals. Thus, the transmitted signal vector emanating from the antennas is depicted by:

$$\mathbf{x}_l = \mathbf{W}_{\mathrm{r},l}\mathbf{P}_{\mathrm{r}}\Phi. \tag{4}$$

Here, $\Phi = [\phi_1, \phi_2, \cdots, \phi_T]^T$ denotes a collection of T orthogonal baseband waveforms [21]. The matrix $\mathbf{P}_{\mathrm{r}} = \mathrm{diag}(\sqrt{P_{\mathrm{r},1}/N_{\mathrm{r}}}, \sqrt{P_{\mathrm{r},2}/N_{\mathrm{r}}}, \ldots, \sqrt{P_{\mathrm{r},T}/N_{\mathrm{r}}})$ governs the power distribution towards each target. Additionally, $\mathbf{W}_{\mathrm{r},l} \in \mathbb{C}^{N_{\mathrm{r}}\times T}$ is the radar's precoding matrix for the l-th signal instance. To optimize radar performance or meet specific radar covariance metrics, this matrix can be adapted. For example, a desired radar covariance matrix is achievable via the design of the correct precoding matrix, $\mathbf{R}_{\mathrm{w}} \equiv \frac{1}{L}\mathbf{W}_{\mathrm{r}} \times \mathbf{W}_{\mathrm{r}}^H = \mathbf{I}_{N_{\mathrm{r}}\times N_{\mathrm{r}}}$, typically reserved for omni-directional radar setups.

The radar returns from all targets are processed using a bank of matched filters aligned with the signal waveform $\phi_t : \forall t = 1, 2, \ldots, T$, each tuned to a specific radar angular-range-Doppler bin. Owing to the orthogonality condition $\phi_t \perp \phi_i : \forall t \neq i$, radar returns from distinct targets are isolatable, enabling the independent detection of each. The associated binary hypothesis challenge for each target is represented as $\mathcal{H}_q : \forall q \in 0, 1$, where $q = 0$ indicates target absence, and $q = 1$ indicates its presence. In mathematical terms, the received radar signal from target t under the hypothesis $\mathcal{H}_q$ is expressed as,

$$\mathbf{y}_{\mathrm{r},t,l|\mathcal{H}_q} = \sqrt{\frac{P_{\mathrm{r},t}}{N_{\mathrm{r}}}} d_{\mathrm{r},t}^{-\eta/2}\, \alpha_t\, \mathbf{A}\left(\theta_{\mathrm{t}}\right) \mathbf{w}_{\mathrm{r},t,l}\, q + \mathbf{n}_{\mathrm{r},l}, \tag{5}$$

where $d_{\mathrm{r},t}^{-\eta}$ is the two-way channel pathloss from BS to the target and backwards with $d_{\mathrm{r},t}$ is the two-way distance, α_t represents the target cross-section, and $\mathbf{A}\left(\theta_t\right) = \mathbf{a}_{\mathrm{T}}\left(\theta_t\right) \times \mathbf{a}_{\mathrm{R}}\left(\theta_t\right)$ is the equivalent array manifold with $\mathbf{a}_{\mathrm{T}}\left(\theta_t\right)$ and $\mathbf{a}_{\mathrm{R}}\left(\theta_t\right)$ represent the transmit and receive steering vector for the t-th target, respectively. In this paper, it is assumed that $\mathbf{a}\left(\theta_t\right) \triangleq \mathbf{a}_{\mathrm{T}}\left(\theta_t\right) = \mathbf{a}_{\mathrm{R}}\left(\theta_t\right)$. After employing interference cancellation (IC) at BS, assuming perfect IC we are left only with the noise term $\mathbf{n}_{\mathrm{r},l} \sim \mathcal{CN}\left(0, 2\sigma_{n_{\mathrm{r}}}^2 \mathbf{I}_{N_{\mathrm{r}}}\right)$, essentially removing the clutter from the communication system.

III. Kullback–Leibler divergence

In this section, we derive the KLD for the separated deployment presented in the previous section. For multivariate Gaussian distributed variables with mean vectors μ_m and μ_n, and associated covariance matrices Σ_m and Σ_n, the KLD is given as:

$$\mathrm{KLD}_{n\to m} = \frac{1}{2\ln 2}\Big(\mathrm{tr}\left(\Sigma_n^{-1}\Sigma_m\right) - 2 + \left(\mu_n - \mu_m\right)^T \times\Sigma_n^{-1}\left(\mu_n - \mu_m\right) + \ln\frac{|\Sigma_n|}{|\Sigma_m|}\Big). \tag{6}$$

This equation plays a crucial role in our derivations of the KLD for the radar systems.

A. KLD for Communication System

The derived KLD for the communication system is based on the case of ZF precoding, where the precoding matrix was given in the section introducing the communication system. The derived KLD expression is applicable to any type of constellations and has been modified to account for the long-term pathloss effect as follows,

$$\mathrm{KLD}_{\mathrm{c},k} = \frac{\lambda\, \alpha_{\mathrm{ZF}}^2\, P_{\mathrm{c},k}\, d_{\mathrm{c},k}^{-\eta}}{2\, M\,(M-1)\left(P_{\mathrm{r}}\, \sigma_F^2\, d_{\mathrm{c},k}^{-\eta} + \sigma_n^2\right)\ln 2}, \tag{7}$$

where M is the modulation order, $\alpha_{\mathrm{ZF}} = \sqrt{N_{\mathrm{c}} - K + 1}$ is the normalisation factor for ZF precoding, and λ is a constant that depends on the constellation, for example, in the case of M-ary Phase Shift Keying (M-PSK) it would be $\lambda_{\mathrm{MPSK}} = M^2$.

B. KLD for Radar System

Given L collected snapshots, the received signal matrix can be expressed as,

$$\mathbf{Y}_{\mathrm{r},t|\mathcal{H}_q} = \sqrt{\frac{P_{\mathrm{r},t}}{N_{\mathrm{r}}}}\alpha_t \mathbf{A}\left(\theta_t\right)\mathbf{W}_{\mathrm{r},t}\, q + \tilde{\mathbf{\Omega}}_{\mathrm{r}}, \tag{8}$$

where $\mathbf{W}_{t,\mathrm{r}} \in \mathbb{C}^{N\times L} = [\mathbf{w}_{t,\mathrm{r},1}, \mathbf{w}_{t,\mathrm{r},2}, \cdots, \mathbf{w}_{t,\mathrm{r},l}]$ and $\tilde{\mathbf{\Omega}}_{\mathrm{r}} \in \mathbb{C}^{N\times L} = [\tilde{\omega}_{t,\mathrm{r},1}, \tilde{\omega}_{t,\mathrm{r},2}, \cdots, \tilde{\omega}_{t,\mathrm{r},l}]$. By noting that $\mathbf{y}_{\mathrm{r},t,l|H_{\mathrm{q}}} \sim \mathcal{CN}\left(\sqrt{\frac{P_{\mathrm{r}}}{N_{\mathrm{r}}}}\alpha_t \mathbf{A}\left(\theta_t\right)\mathbf{w}_{\mathrm{r},t,l}\,\mathrm{q}, 2\sigma_{\tilde{\omega}_{\mathrm{r}}}^2 \mathbf{I}_N\right)$. By multiplying the received signal vector with the Hermitian of the known precoding vector and averaging over L, we obtain the matrix $\mathbf{E}_t \in \mathbb{C}^{N_{\mathrm{r}}\times N_{\mathrm{r}}}$,

$$\mathbf{E}_t = \frac{1}{L}\sum_{l=1}^{L}\mathbf{y}_{\mathrm{r},t,l|H_1}\mathbf{w}_{\mathrm{r},t,l}^H. \tag{9}$$

Then we can combine the different signals from each antenna obtaining ξ_t as follows,

$$\xi_t = \frac{\mathbf{a}^H\left(\theta_t\right)\mathbf{E}_t\mathbf{a}\left(\theta_t\right)}{N_{\mathrm{r}}}, \tag{10}$$

Considering a perfect estimation of α_t and θ_t, by assuming that $L \to \infty$. Substituting for $\mathbf{y}_{\mathrm{r},t,l|H_1}$ using (5) we get,

$$\xi_t = \sqrt{\frac{P_{\mathrm{r},t}}{N_{\mathrm{r}}}}\, d_{\mathrm{r},t}^{-\eta}\, \alpha_t \mathbf{a}\left(\theta_t\right)^T \mathbf{R}_t \mathbf{a}\left(\theta_t\right) + \breve{n}_{\mathrm{r}}, \tag{11}$$

where $\breve{n}_{\mathrm{r}} \sim \mathcal{CN}\left(0, 2\sigma_{n_{\mathrm{r}}}^2\right)$, and $\mathbf{R}_t = \frac{1}{L}\sum_{l=1}^{L}\mathbf{w}_{\mathrm{r},t,l}\,\mathbf{w}_{\mathrm{r},t,l}^H$. The KLD can be derived from (11) using the KLD for multivariate Gaussian from (6), where $\Sigma_n = \Sigma_m = \sigma_{n_{\mathrm{r}}}^2$, $\mu_n = 0$, and $\mu_m = \sqrt{\frac{P_{\mathrm{r},t}}{N_{\mathrm{r}}}}\, d_{\mathrm{r},t}^{-\eta}\, \alpha_t \mathbf{a}_{\mathrm{T}}\left(\theta_t\right)^T \mathbf{R}_t \mathbf{a}_{\mathrm{T}}\left(\theta_t\right)$ for $\mathrm{KLD}_{0\to 1}$, the same $\mathrm{KLD}_{1\to 0}$ can be formulated. The resultant $\mathrm{KLD}_{\mathrm{r,t}} = (\mathrm{KLD}_{0\to 1}$+$\mathrm{KLD}_{1\to 0})/2$ will be as follows,

$$\mathrm{KLD}_{\mathrm{r,t}} = \frac{|\alpha_t|^2\, d_{\mathrm{r},t}^{-\eta}\, P_{\mathrm{r},t}\, |\mathbf{a}^H(\theta_t)\,\mathbf{R}_t\,\mathbf{a}(\theta_t)|^2}{2\, N_{\mathrm{r}}\, \sigma_n^2 \ln 2}. \tag{12}$$

By considering the derived KLD for all radar targets and all served communication UEs, the weighted average KLD for the overall Radcom network can be formulated as

$$\mathrm{KLD}_{\mathrm{avg}} = \left(\mathrm{c}_{\mathrm{com}}\sum_{k=1}^{K}\mathrm{KLD}_{\mathrm{c},k} + \mathrm{c}_{\mathrm{rad}}\sum_{t=1}^{T}\mathrm{KLD}_{\mathrm{r},t}\right), \tag{13}$$

where $\mathrm{c_{com}}$ and $\mathrm{c_{rad}}$ are the weights for each system, with $K\,\mathrm{c_{com}} + T\,\mathrm{c_{rad}} = 1$. The weights gives priority to the desired system which allows for more flexibility and trade-off.

IV. Numerical Results

In this section, we present the performance analysis and trade-offs between $\mathrm{KLD_c}$ and $\mathrm{KLD_r}$, where $\mathrm{KLD_c} = \mathrm{c_{com}} \sum_{k=1}^{K} \mathrm{KLD_{c,}}_k$ and $\mathrm{KLD_r} = \mathrm{c_{rad}} \sum_{t=1}^{T} \mathrm{KLD_{r,}}_t$. The system scenario considered in the simulations is a multi-user-multi-target scenario, where a number of 2 UEs and 2 targets have been considered for separated antenna deployment. The antenna separation is set to half wavelength, the total transmit power is fixed at $P_{\mathrm{T}} = 1$, the covariance matrix for the radar in the case of separated deployment is $\mathbf{R}_x = \mathbf{I}_{N_{\mathrm{r}}}$, the target cross section is normalised to $\alpha_t = 1\ \forall t$, and QPSK modulation is used throughout the results. In addition, the pathloss exponent is set to $\eta = 3$ which is considered to model the effect of large-scale fading, and the total number of antennas at BS is fixed at $N = 20$ where the antennas are uniformly allocated for each subsystem $N_c = 10$, and $N_r = 10$. The distances between the BS and each UE are 270, and 80, respectively. The distances between the BS and each target are 380 and 110, respectively, with θ_t equal to 35° and 125° for each target.

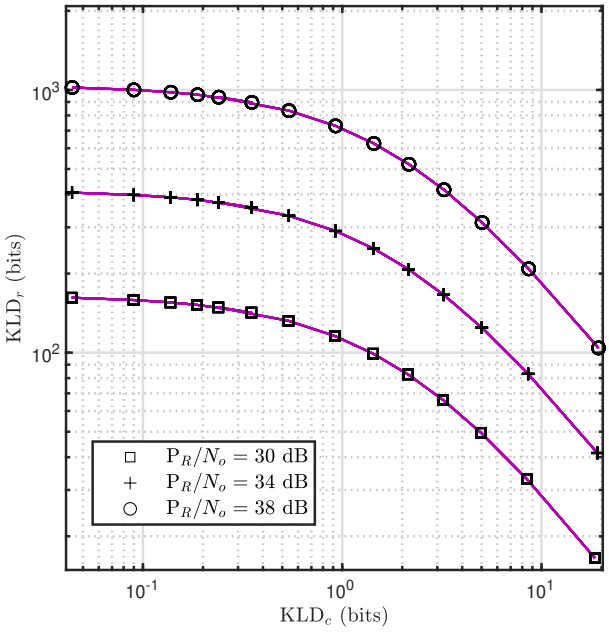

Fig. 2. $\mathrm{KLD_c}$ versus $\mathrm{KLD_r}$ trade-off for separated antenna deployment done for different values of $\mathrm{P_R}/N_o$

In Fig.2, the trade-off is shown between the $\mathrm{KLD_c}$ versus $\mathrm{KLD_r}$, where the P_{r} is ranged from 0 to 1, where $P_{\mathrm{c}} = P_{\mathrm{T}} - P_{\mathrm{r}}$ and the weights is fixed at $\mathrm{c_{com}} = \mathrm{c_{rad}} = \frac{1}{K+T}$, showing the effect of varying the power and how it reflects on the performance of each system. Here we notice that the power can be utilized to provide maximal trade-off between the two systems as more power allocated to either system will give it more performance.

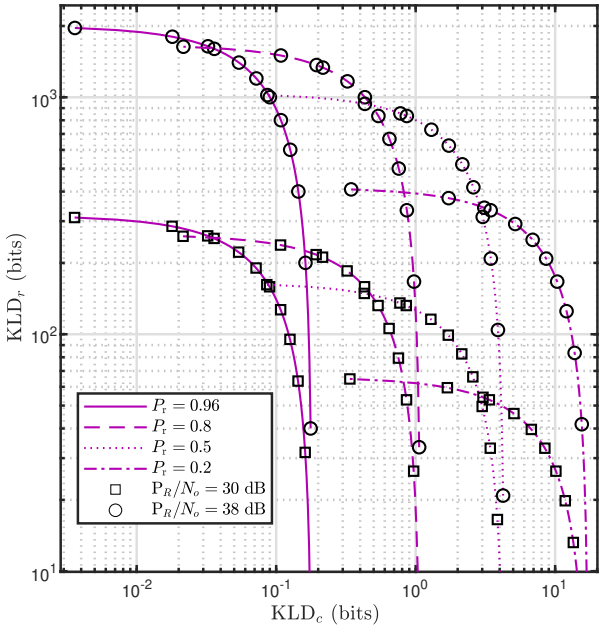

Fig. 3. $\mathrm{KLD_c}$ versus $\mathrm{KLD_r}$ trade-off for the separated antenna deployment done for different values of $\mathrm{P_R}/N_o$

In Fig.3, the trade-off for separated antenna deployment here is shown for fixed powers but variable weights, where the P_{r} is ranged from 0 to 1, where $P_{\mathrm{c}} = P_{\mathrm{T}} - P_{\mathrm{r}}$ and the weights are varied by varying $\mathrm{c_{com}}$ from 0 to $\frac{2}{T+K}$, calculating $\mathrm{c_{rad}}$ using $\mathrm{c_{rad}} = \frac{1-K\,\mathrm{c_{com}}}{T}$. This shows the effect of varying the weights and how it reflects on the performance of each system. It is important to note that the communication system have more interference due to the absence of IC at the UE side, therefore, it is noticed that more power needs to be allocated towards the communication system in order to provide same performance trade-off, unlike the radar system.

In Fig.4, the trade-off for separated antenna deployment here shows the relation of power to symbol error rate for communication subsystem and probability of detection for the radar subsystem. The power is varied for the subsystem, showing the effect on the combined symbol error rate for both UEs, and the combined detection probability for both targets. Here, we see in Fig.4.a, shows that the communication system increase in performance in terms of symbol error rate for the UEs when P_{c} increases. This is as a result of reducing the effect of the radar interference as P_{T} is fixed, which increases the performance of the communication system.

In Fig.4.b, also shows the increase in radar system performance when P_{r} increases, here the system does IC so the only performance reduction is due to the decrease in power for the radar, this is important to note, as the radar system has the edge of using the BS capabilities while the UEs are battery limited devices.

V. Conclusion

In this paper, we proposed the utilization of the KLD as a unifying measure for both subsystems into one integrated Radcom system. The KLD metric offers a streamlined ap-

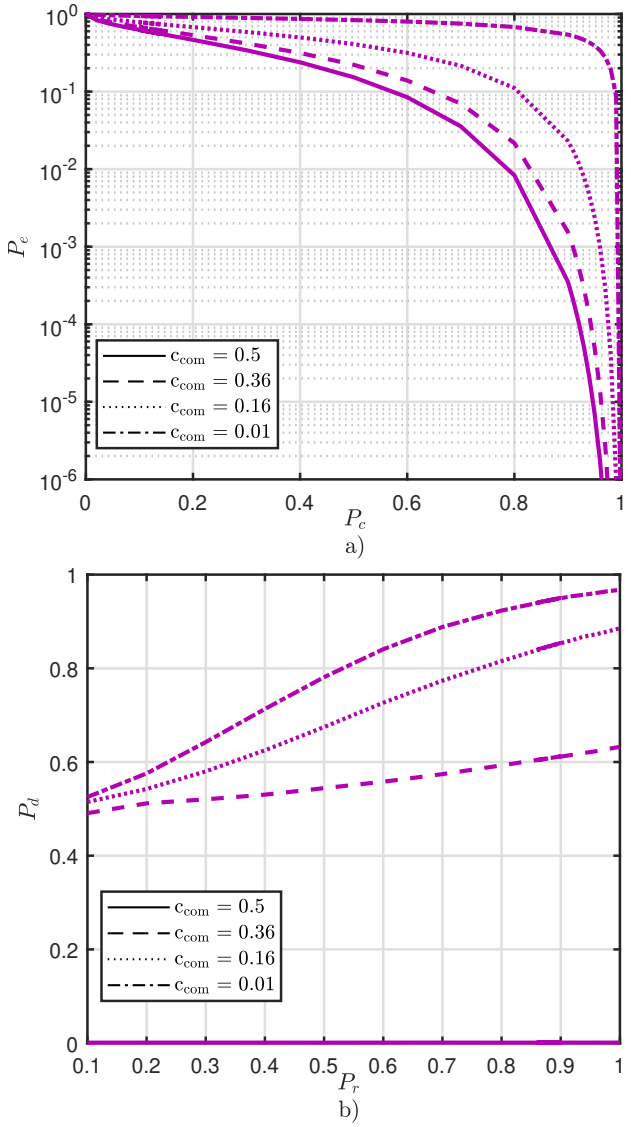

Fig. 4. a) Symbol error rate versus P_c; b) Probability of detection P_d versus P_c for different values of weights for each subsystem

proach to Radcom design, enhancing efficiency and facilitating clear observation and control of the trade-offs between the two subsystems.

The trade-offs between the two subsystems in RadCom is analyzed for separated antenna deployment configuration using the derived unified KLD for the radar system. The results clearly indicated that the separated antenna deployment shows promising results with a highly flexible and controllable system using the unified KLD measure for both subsystems. This underscores the potential advantages of the KLD and the separated deployment approach for future Radcom systems. Future research could explore the impact of imperfect interference cancellation on the KLD metric and the resulting trade-offs.

REFERENCES

[1] I. F. Akyildiz, A. Kak, and S. Nie, "6G and beyond: The future of wireless communications systems," *IEEE Access*, vol. 8, pp. 133 995–134 030, 2020.

[2] M. Giordani, M. Polese, M. Mezzavilla, S. Rangan, and M. Zorzi, "Toward 6G networks: Use cases and technologies," *IEEE Commun. Mag.*, vol. 58, no. 3, pp. 55–61, 2020.

[3] M. Z. Chowdhury, M. Shahjalal, S. Ahmed, and Y. M. Jang, "6G wireless communication systems: Applications, requirements, technologies, challenges, and research directions," *IEEE Open J. Commun. Soc.*, vol. 1, pp. 957–975, 2020.

[4] N. Rajatheva, I. Atzeni, E. Bjornson, A. Bourdoux, S. Buzzi, J.-B. Dore, S. Erkucuk, M. Fuentes, K. Guan, Y. Hu, X. Huang, J. Hulkkonen, J. M. Jornet, M. Katz, R. Nilsson, E. Panayirci, K. Rabie, N. Rajapaksha, M. Salehi, H. Sarieddeen, T. Svensson, O. Tervo, A. Tolli, Q. Wu, and W. Xu, "White paper on broadband connectivity in 6G," *arXiv preprint arXiv:2004.14247*, 2020. [Online]. Available: https://doi.org/10.48550/arXiv.2004.14247

[5] F. Liu, C. Masouros, A. Li, and T. Ratnarajah, "Robust MIMO beamforming for cellular and radar coexistence," *IEEE Wireless Commun. Lett.*, vol. 6, no. 3, pp. 374–377, 2017.

[6] F. Liu, L. Zhou, C. Masouros, A. Li, W. Luo, and A. Petropulu, "Toward dual-functional radar-communication systems: Optimal waveform design," *IEEE Trans. Signal Process.*, vol. 66, no. 16, pp. 4264–4279, 2018.

[7] A. Liu, Z. Huang, M. Li, Y. Wan, W. Li, T. X. Han, C. Liu, R. Du, D. K. P. Tan, J. Lu, Y. Shen, F. Colone, and K. Chetty, "A survey on fundamental limits of integrated sensing and communication," *IEEE Commun. Surveys Tuts.*, vol. 24, no. 2, pp. 994–1034, 2022.

[8] M. Temiz, E. Alsusa, and M. W. Baidas, "A dual-functional massive MIMO OFDM communication and radar transmitter architecture," *IEEE Trans. Veh. Technol.*, vol. 69, no. 12, pp. 14 974–14 988, 2020.

[9] ——, "Optimized precoders for massive MIMO OFDM dual radar-communication systems," *IEEE Trans. Commun.*, vol. 69, no. 7, pp. 4781–4794, 2021.

[10] J. A. Zhang, F. Liu, C. Masouros, R. W. Heath, Z. Feng, L. Zheng, and A. Petropulu, "An overview of signal processing techniques for joint communication and radar sensing," *IEEE J. Sel. Topics Signal Process.*, vol. 15, no. 6, pp. 1295–1315, 2021.

[11] M. Al-Jarrah, E. Alsusa, and C. Masouros, "A unified performance framework for integrated sensing-communications based on KL-Divergence," *IEEE Trans. Wireless Commun.*, pp. 1–1, 2023.

[12] Y. Kloob, M. Al-Jarrah, E. Alsusa, and C. Masouros, "Novel KLD-based Resource Allocation for Integrated Sensing and Communication," *IEEE Trans. Signal Process.*, pp. 1–15, 2024.

[13] B. Tang, M. M. Naghsh, and J. Tang, "Relative entropy-based waveform design for MIMO radar detection in the presence of clutter and interference," *IEEE Trans. Signal Process.*, vol. 63, no. 14, pp. 3783–3796, 2015.

[14] J. Tang, N. Li, Y. Wu, and Y. Peng, "On detection performance of MIMO radar: A relative entropy-based study," *IEEE Signal Process. Lett.*, vol. 16, no. 3, pp. 184–187, 2009.

[15] N. Fatema, G. Hua, Y. Xiang, D. Peng, and I. Natgunanathan, "Massive MIMO linear precoding: A survey," *IEEE Syst. J.*, vol. 12, pp. 3920–3931, 2018.

[16] Y. Zhang, L. Wang, J. Tang, and J. Pan, "Multi-hypothesis test for close targets detection in co-located MIMO radar," *The Journal of Engineering*, vol. 2019, no. 19, pp. 5986–5989, 2019. [Online]. Available: https://ietresearch.onlinelibrary.wiley.com/doi/abs/10.1049/joe.2019.0456

[17] H. Zhang, J. Shi, Q. Zhang, B. Zong, and J. Xie, "Antenna selection for target tracking in collocated MIMO radar," *IEEE Trans. Aerosp. Electron. Syst.*, vol. 57, no. 1, pp. 423–436, 2021.

[18] A. Zaimbashi, "Forward M-Ary hypothesis testing based detection approach for passive radar," *IEEE Trans. on Signal Process.*, vol. 65, no. 10, pp. 2659–2671, 2017.

[19] L. Wang, W. Zhu, Y. Zhang, Q. Liao, and J. Tang, "Multi-target detection and adaptive waveform design for cognitive MIMO radar," *IEEE Sensors J.*, vol. 18, no. 24, pp. 9962–9970, 2018.

[20] W. Yi, T. Zhou, Y. Ai, and R. S. Blum, "Suboptimal low complexity joint multi-target detection and localization for non-coherent MIMO radar with widely separated antennas," *IEEE Trans. Signal Process.*, vol. 68, pp. 901–916, 2020.

[21] A. Hassanien and S. A. Vorobyov, "Phased-MIMO radar: A tradeoff between phased-array and MIMO radars," *IEEE Trans. Signal Process.*, vol. 58, no. 6, pp. 3137–3151, 2010.